Substituent-sensitive fluorescence of sequentially N-alkylated tetrabenzotetraaza[8]circulenes

Gleb V. Baryshnikov,*[ab] Rashid R. Valiev,[acd] Boris F. Minaev,[bc] Hans Ågren[ae]

[a]*Division of Theoretical Chemistry and Biology, School of Biotechnology, KTH Royal Institute of Technology, 10691 Stockholm, Sweden.*
E-mail: glibar@kth.se
[b]*Department of Chemistry and Nanomaterials Science, Bogdan Khmelnitsky National University, Cherkasy, 18031, Ukraine*
[c]*Tomsk State University, 36 Lenin Avenue, Tomsk, Russia*
[d]*Tomsk Polytechnic University, 43a Lenin Avenue, Tomsk, Russia*
[e]*Institute of Nanotechnology, Spectroscopy and Quantum Chemistry, Siberian Federal University, Svobodny pr. 79, 660041 Krasnoyarsk, Russia*

Abstract

We explore the use of substituent-sensitive balance between fluorescence and non-radiative decay as a tool for optical tuning of promising materials for organic light emitting diode applications. A series of N-butylated tetrabenzotetraaza[8]circulenes are studied computationally in order to explain the gradual decrease of fluorescence intensity with the rise of the substituent number. The inter-system crossing probability is found to increase upon the gradual substitution of the circulene macrocycle as a result of a decrease of the S_1–T_1 energy gap due to the deformation of the tetrabenzotetraaza[8]circulenes and thereby a distortion of the π-conjugation within the macrocycles. In contrast, the S_1–T_1 spin-orbit coupling matrix elements are quite insensitive to the number of outer substituents. As a result, the fluorescence-responsible ππ* transition becomes less intense and the fluorescence rate constant decreases.

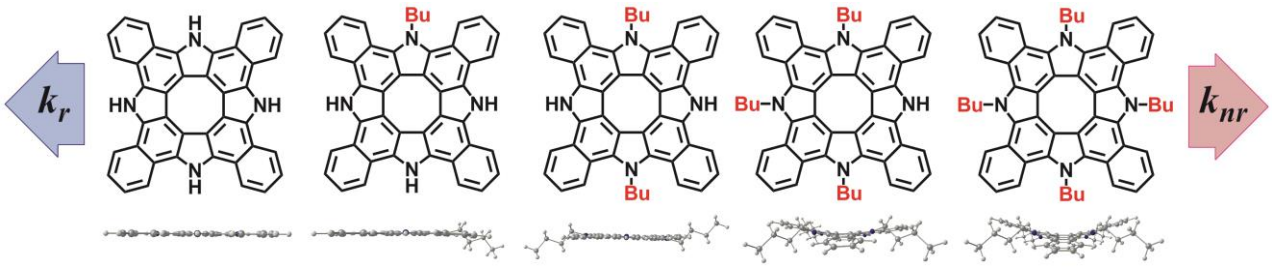

Graphical abstract

1. Introduction

Hetero[8]circulenes have attracted great attention during the last few years due to their promising luminescence properties together with their high stability and low-cost synthetic pathways [1, 2]. The most intriguing application of hetero[8]circulenes is their use as active layers in the cheep and high-stable organic light-emitting diodes (OLEDs) [3–5]. Among a wide family of hetero[8]circulenes the most efficient emitters are benzoannelated unsymmetrical azaoxa[8]circulenes synthesized for the first time by Pittelkow et al. in 2013 [6, 7]. In 2015, Osuka et al. prepared a stand-alone tetrabenzotetraaza[8]circulene (TBTAC) [8] which shows a quite intense fluorescence (φ_{fl} = 0.59) despite the high molecular symmetry (D_{4h} point group). Almost simultaneously Pittelkow et al. [9] presented a synthesis of new unsymmetrical azaoxa[8]circulenes which demonstrated unusual photophysical properties depending on the substitution and benzoannelation effects. In a series of recent papers [4, 10] we have explained Osuka's [8] and Pittelkow's [9] experimental spectroscopic data using specially parameterized semi-empirical schemes and *ab initio* methods for the proper estimation of rate constants for radiative and non-radiative processes. We have also predicted some new azaoxa[8]circulenes [4] which possess outstanding emissive properties due to a purposeful balancing manipulation between radiative and non-radiative deactivation channels. Finally, in the most recent publication, Osuka et. al. [11] presented a synthetic protocol and detailed spectroscopic characterization for a series of novel N-alkylated tetrabenzotetraaza[8]circulenes which demonstrated a substituent-dependent fluorescence behavior. Particularly, the fluorescence quantum yield (Φ_{fl}) gradually decreases from 0.59 for the unsubstituted TBTAC compound to 0.35 for the *tetra*-butyl-TBTAC derivative [11]. At a first glance this seems to be strange because σ-

coupled substituents usually do not strongly affect the photophysical properties of polyaromatic compounds the spectroscopy of which owes to the low-lying ππ*-states. However, a more detailed characterization of the N-butylated TBTAC species by X-ray crystallography indicated that inclusion of three and four Bu-substituents provides a quite strong distortion of the circulene macrocycle that could imply a decrease of fluorescence efficiency. Considering this qualitative statement we present in this work a quantitative spectroscopic characterization for the series of five TBTAC-based compounds (unsubstituted TBTAC molecule and *mono-*, *para-di-*, *tri-*, *tetra-* N-butylated-TBTAC) by means of high-level *ab initio* computations of excited states energies, transitions intensities and spin-orbit coupling (SOC) effects. The present study represents a continuation of our recent work on the purposeful optical tuning of hetero[8]circulenes as fluorescent OLED components [4, 10].

2. Computational details

2.1. Structure and spectroscopic characterization

The ground state optimization for all studied compounds has been carried out by the B3LYP/6-31G(d) method [12-14] in a vacuum approximation with the GAUSSIAN 09 package [15]. The starting-point orientation of the Bu substituents relative to the TBTAC molecular plane has been taken from the X-ray crystallography data [11]. Hessian calculations indicate that optimized conformations of the studied species correspond to genuine minima on the potential energy surfaces at the employed level of theory.

The excitation energies of the first excited singlet state (S_1) and of four lowest-lying triplet excited states (T_1–T_4) were calculated within extended multi-configurational quasi-degenerate second-order perturbation theory (XMC-QDPT2) [16] using the 6-31G(d) basis set and (10,10) complete active space (CAS, 10 electrons and 10 orbitals were included). State averaged calculations were performed over the eight electronic states (4 singlet and 4 triplet states). The effective Hamiltonian of the CASPT2 scheme included here 30 states. The oscillator strength values for the $S_0 \rightarrow S_1$ transitions were also calculated by the XMC-QDPT2/6-31G(d)

method. The SOC matrix elements of the one-electron Breit-Pauli operator were estimated using the CASSCF(10,10) wave functions and the XMC-QDPT2/6-31G(d) electronic states energies. All the XMC-QDPT2 and MCSCF calculations were performed using the Firefly software package [17].

2.2. Photophysical constants

The fluorescence quantum yield (Φ_{fl}^{theor}) [18, 19] can be easily estimated through the main photophysical constants by the following relationship:

$$\Phi_{fl}^{theor} = \frac{k_r}{k_r + k_{IC} + \sum_n k_{S_1T_n}}, \quad (1)$$

where k_r is the radiative rate constant of the electronic transition between the first excited singlet state (S_1) and the ground electronic state (S_0), $k_{S_1T_n}$ is the rate constant of intersystem crossing (ISC) between the first excited singlet state (S_1) and the triplet state (T_n) with the energy lower than the first excited S_1 state, and k_{IC} is the rate constant for the internal conversion between S_1 and S_0 states. Generally, when the energy gap between S_1 and S_0 is higher than 20000 cm^{-1} and the electronic transition $S_1 \rightarrow S_0$ is strongly dipole-allowed the following inequalities are valid [20–22]:

$$k_{IC} << k_{S_1T_i} \text{ and } k_{IC} << k_r \quad (2)$$

In a few recent papers we have shown that the inequalities (2) are also valid for a wide number of substituted and unsubstituted aza- oxa- and azaoxa[8]circulenes [4, 10]. We have found that the k_{IC} term in Eq. (1) is negligibly small for such circulenes and therefore that the Φ_{fl}^{theor} values could be estimated only through the k_r and $k_{S_1T_i}$ rate constants with reasonable accuracy relative to experimental data [10].

The k_r values for the studied TBTAC species were calculated using the well-known equation [18]:

$$k_r = \frac{1}{1.5003} f \cdot E^2, \quad (3)$$

where f and E (cm^{-1}) are the oscillator strength and de-excitation energy of the $S_1 \rightarrow S_0$ electronic transition, respectively (estimated at the XMC-QDPT2 level of theory in

this work). We here approximate $E_{S_1 \to S_0} = E_{S_0 \to S_1}$ that was shown to be an acceptable scheme for azaoxa[8]circulenes and related systems [4, 10, 23]. In accordance to the Franck-Condon (FC) approximation the $k_{S_1T_n}$ values for S-T transitions between $\pi\pi^*$-type electronic states in organic molecules can be estimated by the empirical Eq. 4 [20, 21]:

$$k_{S_1T_n} = 10^{10} \cdot \sum_n \sum_{i,j} \left| \left\langle \Psi_{S_1} \left| H_{SO} \right| \Psi_{T_n} \right\rangle \right|^2 \cdot F_{ij}, \qquad (4)$$

where $\left\langle \Psi_{S_1} \left| H_{SO} \right| \Psi_{T_n} \right\rangle$ are the spin-orbit coupling matrix elements (in cm^{-1}) between the S_1 state and the *n*-th excited triplet state (T_n) lying below the S_1 level, F_{ij} is the FC factor for which *i* and *j* indices refer to the vibrational quantum numbers of the S_{1i} and T_{nj} vibronic states; 10^{10} $cm^2 s^{-1}$ is a fitting parameter which includes $\rho_E/\hbar$ estimation where ρ_E is a typical density of states. It has been previously shown [4, 10, 22] that the F_{ij} factor can be calculated in the harmonic approximation with account of only a single promotive mode ~1400 cm^{-1} for organic compounds which corresponds to C-C stretching vibrations. Of course, such a single-mode approximation is quite rough relative to the more elegant estimations through the FC weighted density of states (FCWDOS) [24–28]. However, for a wide number of organic systems (including azaoxa[8]circulenes) this crude approximation with only one promotive mode has provided reasonable k_{ST} estimations [4,10, 22, 29-33]. The FC factor between the zero vibrational level of the S_1 state and the *j*-th vibrational level of the triplet state can therefore be written as [20, 21]:

$$F_{0j} = \frac{e^{-y} y^j}{j!}, \qquad (5)$$

where $j = \frac{E_{ST}}{1400}$ and it rounded up to an integer, $y = 0.3$ is a dimensionless parameter which represents the shift of equilibrium positions of the normal modes.

3. Results and discussion

3.1. Structural peculiarities

The structures of the five studied TBTAC compounds are presented in Figure 1. Compound **1** actually corresponds to the unsubstituted TBTAC molecule which was synthesized and well characterized both experimentally and theoretically in a series of previous studiess [4, 8]. As follows from the X-ray data and quantum-chemical simulations the TBTAC molecule possesses a strictly planar structure which belongs to the D_{4h} symmetry point group. Bond alternation in the *hub* cyclooctatetraene (COT) core is quite weak (C–C basic pyrrole bonds are only 0.005 Å longer than the neighboring benzene-basic C–C bonds) and does not change upon gradual butylation.

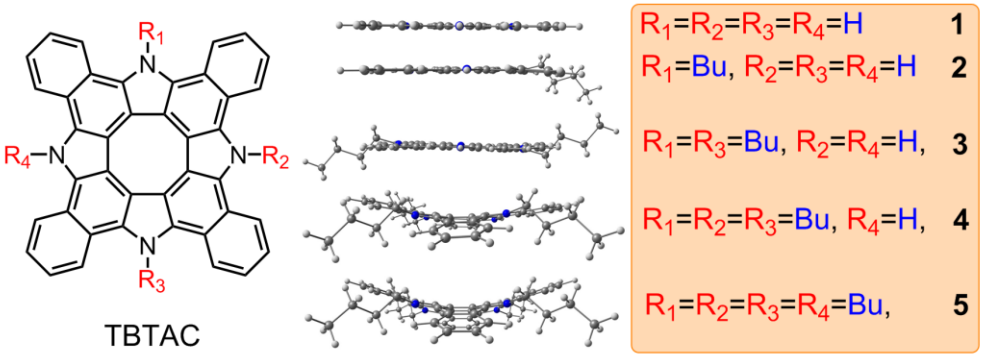

Figure 1. The chemical structure and side-view optimized conformation for the TBTAC molecule **1** and its N-butylated derivatives **2-5.**

Upon mono- (**2**) and *para*-double (**3**) substitution the initial TBTAC macrocycle does not undergo structural deformations, while for the case of *tri*- and *tetra*-butylated species **4** and **5** a significant bend of the TBTAC frame occurs. The deviation from planarity equals 15º and 19º for molecules **4** and **5**, respectively. This is due to the steric hindrance for the simultaneous orientation of the butyl groups in the narrow surrounding of the rigid naphthalene moieties. The same tendency has also been observed experimentally (by X-ray crystallography) for the crystal-packed compound **5** in which one of the Bu groups was replaced by a benzyl (Bn) substituent (Figure 3 in Ref.[11]). Of course, such structural distortion of the TBTAC macrocycle should significantly affect the energies of the low-lying S_1 and T_1 excited states of $\pi\pi^*$ type which are mainly responsible for the observable spectroscopic behavior. The remaining structural parameters are almost the same for compounds **1**-**5** indicating that the N-butyl substituents do not significantly affect the electronic density

distribution in the TBTAC skeleton. It seems intriguing to explain the reason for the experimentally observed two-times decrease of fluorescence quantum yield moving from unsubstituted TBTAC to *tetra*-Bu-TBTAC along these lines.

3.2. Photophysical properties

As follows from the experimental results presented in Table 1 the energy of the S_1 state level decreases monotonously. This fact is in a good agreement with the XMC-QDPT2 estimated energies of the S_1 state except for compound **3** for which the S_1 energy is slightly lower than that for circulene **4**. The intensity for the corresponding S_0–S_1 transition is almost the same for compounds **1**-**4**, while for the *tetra*-Bu-TBTAC molecule **5** it is two times smaller due to the strong structural distortion of the circulene macrocycle. This fact means that the decreasing of the fluorescence quantum yield in the sequence **1** > **2** > **3** > **4** > **5** originates mainly not from the decreasing of the k_r rate constant, but from the strong increasing of the $k_{S_1T_n}$ ISC rate. The latter effect could be caused by two reasons: i) by the enhancement of the spin-orbit coupling between the S_1 and T_n states (n corresponds to the number of triplets below the S_1 state); ii) by the decrease of S_1-T_n energy gap that produces the higher values of the FC factors (Eqns. 4, 5).

Table 1. The energy of spectroscopically important singlet and triplet states for compounds **1-5** (oscillator strength values for spin-allowed S_0–S_1 and S_0–S_2 transitions are presented in parentheses).

Molecule	$E(S_1)$,[a] cm^{-1}	$E(S_1)_{exp}$, cm^{-1}	$E(S_2)$,[a] cm^{-1}	$E(T_1)$,[a] cm^{-1}	$E(T_2)$,[a] cm^{-1}	$E(T_3)$,[a] cm^{-1}	$E(T_4)$,[a] cm^{-1}
1	27556 (0.44)	24213	30397 (0.64)	23800	24109	25973	27665
2	27375 (0.40)	24038	30132 (0.61)	24126	25661	27523	29285
3	25700 (0.42)	23923	29143 (0.56)	22581	23338	25092	26594
4	26100 (0.41)	23697	29224 (0.53)	23338	24976	26980	28521
5	25330 (0.22)	23640	28716 (0.90)	23900	25730	27504	28375

[a] *The singlet and , triplet states energies and oscillator strengths for the corresponding S-S transitions are presented after the final XMC-QDPT2/6-31G(d) corrections.*

As can be seen from Table 2, the $k_{S_1T_n}$ rate constant is the largest one when it refers to the frontier S_1 and T_1 states, and that the overall tendency is that the $\langle S_1|\mathbf{H_{so}}|T_1\rangle$ matrix element decreases slowly upon the gradual butylation of the TBTAC species. At the same time, the SOC matrix elements between the remaining pairs of the S_1 and T_n states are negligibly small comparing with $\langle S_1|\mathbf{H_{so}}|T_1\rangle$ value due to symmetry reasons. For the unsubstituted TBTAC **1** of the D_{4h} symmetry all the $\langle S_1|\mathbf{H_{so}}|T_n\rangle$ (n=2-4) couplings are strictly equal to zero, but upon the butylation and molecular symmetry distortion these matrix elements become non-zero but still remain very small. Actually, the $k_{S_1T_1}$ rate constant for all studied TBTAC species determines completely the overall value of "nonradiative" $\sum_n k_{S_1T_n}$ term in Eqn. 1. Moreover, accounting for the inequalities (2), the $k_{S_1T_1}$ rate constant is almost the same as the k_{nr} rate constant because of the internal conversion contribution is negligibly small for the hetero[8]circulenes species [4, 10]. Summing up shortly, for the studied TBTAC species $k_{nr} = \sum_n k_{S_1T_n} \approx k_{S_1T_1}$, because of $k_{S_1T_1}$ contributions strongly dominates over the rest $k_{S_1T_n}$ (n=2–4) terms. As follows from Eqn. 4 the $k_{S_1T_1}$ rate depends on the squared value of $\langle S_1|\mathbf{H_{so}}|T_1\rangle$ which would imply a decrease of the overall k_{nr} term upon the sequential substitution, which, however, is in contradiction with the experimental data [11] and with the final values of the calculated k_{nr} constants (Table 3). This is because the main factor affecting the ISC rate is the energy gap between the S_1 and T_1 state (ΔE_{ST}).

Table 2. The absolute values of SOC matrix elements between the S_1 state and the series of T_n states (n=1-4) for the circulenes **1-5**. The number of triplet states (n) below S_1 and the ΔE_{ST} gap values are also presented.

Molecule	$\langle S_1\|\mathbf{H_{so}}\|T_1\rangle$, cm^{-1}	$\langle S_1\|\mathbf{H_{so}}\|T_2\rangle$, cm^{-1}	$\langle S_1\|\mathbf{H_{so}}\|T_3\rangle$, cm^{-1}	$\langle S_1\|\mathbf{H_{so}}\|T_4\rangle$, cm^{-1}	n	ΔE_{ST}, cm^{-1}
1	1.57	0.00	0.00	0.00	3	4185
2	1.54	0.11	0.23	0.33	2	3249
3	1.42	0.00	0.00	0.12	3	3119
4	1.39	0.11	0.10	0.08	2	2762
5	1.32	0.00	0.01	0.0	1	1430

Table 3. The main photophysical properties of compounds **1**-**5** (experimental data are taken from Ref. [11]).

Molecule	k_r, s^{-1}	k_r^{exp}, s^{-1}	$k_{S_1T_1}$, s^{-1}	$k_{S_1T_2}$, s^{-1}	$k_{S_1T_3}$, s^{-1}	k_{nr}, s^{-1}	k_{nr}^{exp}, s^{-1}	Φ_{fl}^{theor}	Φ_{fl}^{exp}
1	$2.2\cdot10^8$	$1.6\cdot10^8$	$1.8\cdot10^8$	$0.0\cdot10^0$	$0.0\cdot10^0$	$1.8\cdot10^8$	$1.1\cdot10^8$	55%	59%
2	$2.0\cdot10^8$	$1.5\cdot10^8$	$3.8\cdot10^8$	$1.8\cdot10^7$	-	$4.0\cdot10^8$	$1.2\cdot10^8$	33%	57%
3	$1.9\cdot10^8$	$1.4\cdot10^8$	$4.2\cdot10^8$	$0.0\cdot10^0$	$0.0\cdot10^0$	$4.2\cdot10^8$	$1.4\cdot10^8$	31%	51%
4	$1.9\cdot10^8$	$1.3\cdot10^8$	$9.0\cdot10^8$	$3.7\cdot10^7$	-	$7.2\cdot10^8$	$1.8\cdot10^8$	21%	42%
5	$1.0\cdot10^8$	$1.2\cdot10^8$	$37\cdot10^8$	-	-	$37\cdot10^8$	$2.2\cdot10^8$	3%	35%

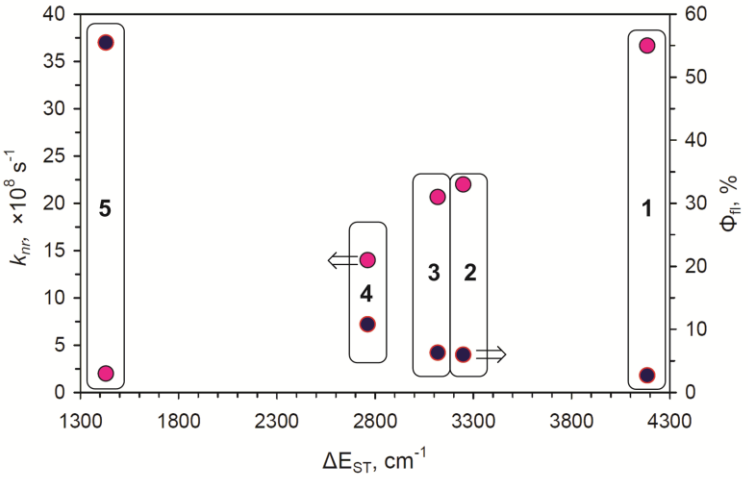

Figure 2. Dependence between the k_{nr} (left axis, red color) and Φ_{fl}^{theor} (right axis, black color) constants *vs.* ΔE_{ST} energy gap for the studied series of sequentially N-butylated tetrabenzotetraaza[8]circulenes **1**-**5**.

One can stress that the calculated values of the fluorescence rate constant are in excellent quantitative agreement with the experimental data [11] indicating a correct estimation for the energy and oscillator strength of S_0–S_1 transition. At the same time our calculations clearly overestimate the rate constant for the nonradiative quenching, something that can be assigned to the limitation of the single-mode approximation for k_{nr}. As a result, the calculated values of Φ_{fl}^{theor} decreases much faster than observed experimentally (Table 3, Figure 2). In fact, the driving force of optical tuning of N-alkylated tetrabenzotetraaza[8]circulenes is the dependence of the ΔE_{ST} gap on the number of outer substituents (Figure 2). It is a quite unusual phenomenon that σ-coupled alkyl substituents affect the disposition of the S_1 and T_1 energy levels so significantly. Moreover, such substituent-dependent emission is an inherent feature not only for the TBTAC-based species but also for the azatrioxa[8]circulenes in general as was reported previously [4,10]. This indicates that σ-substitution is a

simple tool for the control of emission properties of hetero[8]circuelnes without changing of the macrocycle structure. This, of course, owes to the high sensitivity of the π-extended electronic shell of hetero[8]circulenes from the presence of σ-type substituents in the outer perimeter.

We speculate that this effect origins in that the outer substituents perturbs the balance between the diatropic ("aromatic") and paratropic ("antiaromatic") ring currents [10] that naturally affects the energy of the singlets and triplets. However, an explanation for the interconnection between the aromaticity and photophysical constants remains open for polyaromatic compounds. Recently, Cremer and coauthors [34] collected and classified aromaticity descriptors, among them only one descriptor was based on the spectroscopic activity of π-conjugated systems – the so-called AI(vib) criterion – an aromaticity index based on the molecular vibrations [34], Thus relations between photophysics and aromaticity of π-conjugated systems [35] remains yet an unsolved area for future research which will have impact on the further understanding of the currently studied hetero[8]circulenes.

4. Conclusions

In the present work we have computationally studied the photophysical properties of a series of sequentially N-alkylated tetrabenzotetraaza[8]circulenes synthesized recently by Osuka et. al. [8]. The experimentally observed sensitivity of the main photophysical constants – the fluorescence quantum yield (Φ_{fl}), radiative and non-radiative rates – on the number of outer butyl substituents has been explained in terms of energy and intensity of the S_0–S_1 transition and the intersystem coupling between the S_1 and T_n states that lie below S_1 state. The S_1~S_0 internal conversion rates have not been numerically estimated in this work but we assume they are negligibly small based on our previous estimations [4, 10]. The radiative rate constant (k_r) only slightly changes upon the gradual substitution in good agreement with the experimental measurements. The slight decrease of k_r is caused by the structural distortion of the circulene macrocycle due to the substitution which is purely a steric effect. We find that spin-orbit coupling contribution does not significantly affect the values of the non-radiative rate constant and thus contributes

negligibly to the intersystem crossing rate (ISC). Instead, the key factor that affects the Φ_{fl} values is the energy gap between the S_1 and T_1 states that provides higher probabilities of the ISC rate constants. That is, the reason for the increasing contribution of ISC over the fluorescence process and the significant decrease of the Φ_{fl} values upon sequential butylation. This is a clear example of optical tuning through the variation of the ΔE_{ST} gap by σ-type substitution and which is demonstrated here for the hetero[8]circulenes family for the first time. We believe that this phenomenon could be useful for optimizing the optical properties of various hetero[8]circulenes for their future application in OLEDs.

Acknowledgements

The calculations were performed with computational resources provided by the High Performance Computing Center North (HPC2N) which is a Swedish national center for Scientific and Parallel Computing through the project ‘‘Multiphysics Modeling of Molecular Materials” SNIC 2016-34-43. This work was supported by Carl Tryggers foundation (Grant No. CTS 16:536), by the Ministry of Education and Science of Ukraine (project No. 0115U003637) and by the QUAMER project (Tomsk State Univeristy).

References

1. G. V. Baryshnikov, B. F. Minaev and V. A. Minaeva, *Russ. Chem. Rev.*, 2015, **84**, 455.

2. T. Hensel, N. N. Andersen, M. Plesner and M. Pittelkow, *Synlett.*, 2016, **27**, 498.

3. C. B. Nielsen, T. Brock-Nannestad, T. K. Reenberg, P. Hammershøj, J. B. Christensen, J. W. Stouwdam and M. Pittelkow, *Chem. Eur. J.*, 2010, **16**, 13030.

4. G. V. Baryshnikov, R. R. Valiev, N. N. Karaush, V. A. Minaeva, A. N. Sinelnikov, S. K. Pedersen, M. Pittelkow, B. F. Minaev and H. Ågren, *Phys. Chem. Chem. Phys.*, 2016, **18**, 28040.

5. K. B. Ivaniuk, G. V. Baryshnikov, P. Y. Stakhira, S. K. Pedersen, M. Pittelkow, A. Lazauskas, D. Volyniuk, J. V. Grazulevicius, B. F. Minaev and H. Ågren, *J. Mater. Chem. C*, 2017, **5**, 4123.

6. C. B. Nielsen, T. Brock-Nannestad, P. Hammershøj, T. K. Reenberg, M. Schau-Magnussen, D. Trpcevski, T. Hensel, R. Salcedo, G. V. Baryshnikov, B. F. Minaev and M. Pittelkow, *Chem. Eur. J.*, 2013, **19**, 3898.

7. T. Hensel, D. Trpcevski, C. Lind, R. Grosjean, P. Hammershøj, C. B. Nielsen, T. Brock-Nannestad, B. E. Nielsen, M. Schau-Magnussen, B. Minaev, G. V. Baryshnikov and M. Pittelkow, *Chem. Eur. J.*, 2013, **19**, 17097.

8. F. Chen, Y. S. Hong, S. Shimizu, D. Kim, T. Tanaka and A. Osuka, *Angew. Chem. Int. Ed.*, 2015, **54**, 10639.

9. M. Plesner, T. Hensel, B. E. Nielsen, F. S. Kamounah, T. Brock-Nannestad, C. B. Nielsen, C. G. Tortzen, O. Hammerich and M. Pittelkow, *Org. Biomol. Chem.*, 2015, **13**, 5937.

10. G. V. Baryshnikov, R. R. Valiev, B. F. Minaev and H, Ågren, *New J. Chem.*, 2017, **41**, 2717.

11. F. Chen, Y. S. Hong, D. Kim, T. Tanaka and A. Osuka, *ChemPlusChem*, 2016, DOI: 10.1002/cplu.201600537.

12. D. Becke, *Phys. Rev. A: At., Mol., Opt. Phys.*, 1988, **38**, 3098.

13. C. Lee, W. Yang and R. G. Parr, *Phys. Rev. B: Condens. Matter Mater. Phys.*, 1988, **37**, 785.

14. M. M. Francl, W. J. Pietro, W. J. Hehre, J. S. Binkley, D. J. DeFrees, J. A. Pople and M. S. Gordon, *J. Chem. Phys.*, 1982, **77**, 3654.

15. M. J. Frisch, G. W. Trucks, H. B. Schlegel, G. E. Scuseria, M. A. Robb, J. R. Cheeseman, G. Scalmani, V. Barone, B. Mennucci, G. A. Petersson, H. Nakatsuji, M. Caricato, X. Li, H. P. Hratchian, A. F. Izmaylov, J. Bloino, G. Zheng, J. L. Sonnenberg, M. Hada, M. Ehara, K. Toyota, R. Fukuda, J. Hasegawa, M. Ishida, T. Nakajima, Y. Honda, O. Kitao, H. Nakai, T. Vreven, J. A. Montgomery, Jr., J. E. Peralta, F. Ogliaro, M. Bearpark, J. J. Heyd, E. Brothers, K. N. Kudin, V. N. Staroverov, R. Kobayashi, J. Normand, K. Raghavachari, A.Rendell, J.C.Burant, S. S. Iyengar, J. Tomasi, M.Cossi, N.Rega, J. M. Millam, M. Klene, J. E. Knox, J. B. Cross, V. Bakken, C. Adamo, J. Jaramillo, R. Gomperts, R. E. Stratmann, O. Yazyev, A. J. Austin, R. Cammi, C. Pomelli, J. W. Ochterski, R. L. Martin, K. Morokuma, V.

G. Zakrzewski, G. A. Voth, P. Salvador, J. J. Dannenberg, S. Dapprich, A. D. Daniels, O. Farkas, J. B. Foresman, J. V. Ortiz, J. Cioslowski and D. J. Fox, *Gaussian 09, Revision D.01*, Gaussian, Inc., Wallingford, CT, 2013.

16. A. A. Granovsky, *J. Chem. Phys.*, 2011, **134**, 214113.

17. Firefly, Alex A. Granovsky, http://classic.chem.msu.su/gran/gamess/index.html.

18. S. P. McGlynn, T. Azumi and M. Kinoshita, *Molecular spectroscopy of the triplet state*, Englewood Cliffs, New Jersey, 1969, p. 434.

19. V. G. Plotnikov, V. A. Dolgikh and V. M. Komarov, *Opt. Spectrosc.*, 1977, **43**, 522.

20. V. G. Plotnikov, V. A. Dolgikh and V. M. Komarov, *Opt. Spectrosc.*, 1977, **43**, 522.

21 V. G. Plotnikov, *Int. J. Quantum Chem.*, 1979, **16**, 527.

22 R. R. Valiev, V. N. Cherepanov, V. Ya. Artyukhov and D. Sundholm, *Phys. Chem. Chem. Phys.*, 2012, **14**, 11508.

23. N. N. Karaush, R. R. Valiev, G. V. Baryshnikov, B. F. Minaev and H. Agren, *Chem. Phys.*, 2015, **459**, 65.

24. C. M. Marian, *Wiley Interdiscip. Rev.: Comput. Mol. Sci.*, 2012, **2**, 187.

25. M. Etinski, J. Tatchen and C. M. Marian, *J. Chem. Phys*., 2011, **134**, 154105.

26. M. Etinski, V. Rai-Constapel and C. M. Marian, *J. Chem. Phys.*, 2014, **140**, 114104.

27. Y. Niu, Q. Peng, C. Deng, X. Gao and Z. Shuai, *J. Phys. Chem. A*, 2010, **114**, 7817.

28. G. Baryshnikov, B. Minaev and H. Ågren, *Chem. Rev.*, 2017, DOI: 10.1021/acs.chemrev.7b00060.

29. R. R. Valiev, A. N. Sinelnikov, Y. V. Aksenova, R. T. Kuznetsova, M. B. Berezin, A. S. Semeikin and V. N. Cherepanov, *Spectrochim. Acta, Part A*, 2014, **117**, 323.

30. R. R. Valiev, E. N. Telminov, T. A. Solodova, E. N. Ponyavina, R. M. Gadirov, M. G. Kaplunov and T. N. Kopylova, *Spectrochim. Acta, Part A*, 2014, **128**, 137.

31. B. F. Minaev, R. R. Valiev, E. N. Nikonova, R. M. Gadirov, T. A. Solodova and T. N. Kopylova, *J. Phys. Chem. A*, 2015, **119**, 1948.

32. L. G. Samsonova, R. R. Valiev, K. M. Degtyarenko, D. A. Sunchugashev, I. N. Kukhta, A. V. Kukhta and T. N. Kopylova, *Spectrochim. Acta, Part A*, 2017, **173**, 59.
33. B. F. Minaev, S. Knuts, H. Agren, *Chem. Phys.*, 1994, **181**, 15.
34. D. Setiawan, E. Kraka and D. Cremer, *J. Org. Chem.*, 2016, **81**, 9669.
35. G. V. Baryshnikov, B. F. Minaev, M. Pittelkow, C.B. Nielsen, R. Salsedo. *J. Mol. Model.*, 2013, **19**, 847.